Int J Interact Des Manuf
DOI 10.1007/s12008-016-0308-5

ORIGINAL PAPER

Appraisal of open software for finite element simulation of 2D metal sheet laser cut

Daniel Mejia[1,2] · **Aitor Moreno**[1] · **Oscar Ruiz-Salguero**[2] · **Iñigo Barandiaran**[1]

Received: 15 February 2016 / Accepted: 12 March 2016

Abstract FEA simulation of thermal metal cutting is central to interactive design and manufacturing. It is therefore relevant to assess the applicability of FEA open software to simulate 2D heat transfer in metal sheet laser cuts. Application of open source code (e.g. FreeFem++, FEniCS, MOOSE) makes possible additional scenarios (e.g. parallel, CUDA, etc.), with lower costs. However, a precise assessment is required on the scenarios in which open software can be a sound alternative to a commercial one. This article contributes in this regard, by presenting a comparison of the aforementioned freeware FEM software for the simulation of heat transfer in thin (i.e. 2D) sheets, subject to a gliding laser point source. We use the commercial ABAQUS software as the reference to compare such open software. A convective linear thin sheet heat transfer model, with and without material removal is used. This article does not intend a full design of computer experiments. Our partial assessment shows that the thin sheet approximation turns to be adequate in terms of the relative error for linear alumina sheets. Under mesh resolutions better than 10^{-5} m , the open and reference software temperature differ in at most 1 % of the temperature prediction. Ongoing work includes adaptive re-meshing, nonlinearities, sheet stress analysis and Mach (also called 'relativistic') effects.

Keywords Laser machining · Sheet cutting · Heat transfer · Finite element analysis

✉ Aitor Moreno
amoreno@vicomtech.org

[1] Vicomtech-IK4, Mikeletegi Pasealekua, 57, Donostia-San Sebastián, Spain

[2] Laboratorio de CAD CAM CAE, Universidad EAFIT, K49 #7 Sur-50, Medellín, Colombia

Abbreviations

FEM/FEA	Finite element method/finite element analysis
$\mathbf{x},\ t$	Coordinates describing the spatial $[x, y]$ and temporal $t \geq 0$ domain of the simulation ($[m, m]$, s)
$u = u(\mathbf{x}, t)$	Temperature distribution along the sheet at a given time (K)
ρ	Sheet metal density $\left(\frac{\text{kg}}{\text{m}^3}\right)$
c_p	Sheet specific heat capacity $\left(\frac{\text{J}}{\text{kg K}}\right)$
k	Sheet thermal conductivity $\left(\frac{\text{W}}{\text{m K}}\right)$
R	Sheet reflectivity i.e., portion of the laser energy that is not absorbed by the sheet ($0 \leq R \leq 1$)
Δz	Sheet thickness (m)
$q = q(u)$	Heat loss due to convection at the sheet surface $\left(\frac{\text{W}}{\text{m}^2}\right)$
h	Natural convection coefficient of the sheet surrounding medium $\left(\frac{\text{W}}{\text{m}^2\,\text{K}}\right)$
u_∞	Temperature of the sheet surrounding medium (K)
$S = S(\mathbf{x}, t)$	Laser power density distribution along the sheet at a given time $\left(\frac{\text{W}}{\text{m}^3}\right)$
P	Laser power (W)
σ	Gaussian laser model's parameter (m)
$\mathbf{x_0} = \mathbf{x_0}(t)$	Laser spot 2D coordinates $[x_0(t), y_0(t)]$ at a given time ($[m, m]$)
v	Laser scanning speed $\left(\frac{\text{m}}{\text{s}}\right)$
ε	Kerf width of the laser (m)
$u_{ref} = u_{ref}(\mathbf{x}, t)$	Reference temperature used to measure the relative error of a given solution (K). This article considers the temperature

Published online: 21 March 2016

distribution obtained by the ABAQUS software as reference

$E = E(\mathbf{x}, t)$ Relative error distribution of a software approximation w.r.t. u_{ref} along the sheet at a given time

$ME = ME(t)$ Maximum relative error of a software temperature approximation w.r.t. u_{ref} at a given time

1 Mathematical modeling for interactive design and manufacturing

In the last years, the manufacturing landscape is adopting the novel concepts presented under the Industry 4.0 tag [1]. The technologies behind the Industry 4.0 concept allow manufacturers to introduce novel technologies and new relationships across the whole product life cycle: from the very early design stages, the production and the quality control till the recycling. The information flux is not linear anymore, and the feedback comprehension and reutilisation in earlier stages of the production line will enable continuous improvement and optimization of the processes.

In Fig. 1, the main concepts of the Industry 4.0 vision are represented. Although most of the current literature focuses on big data, internet of things, robotics or data exploitation, interactive visual computing is considered a key technology in the new paradigm. Interactive visual computing encloses a variety of interrelated disciplines: computer graphics, computer vision, human–machine interaction and simulation. In addition to this, simulation is also considered part of the new proposed technological framework supporting the transition

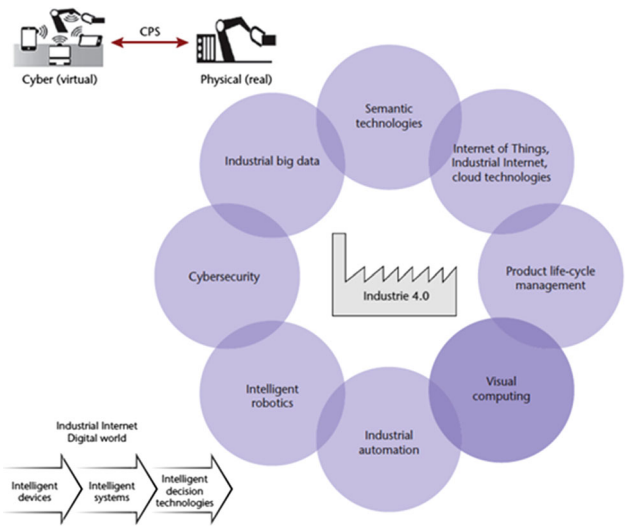

Fig. 1 Visual computing challenges of advanced manufacturing and industrie 4.0 (Ref. [1])

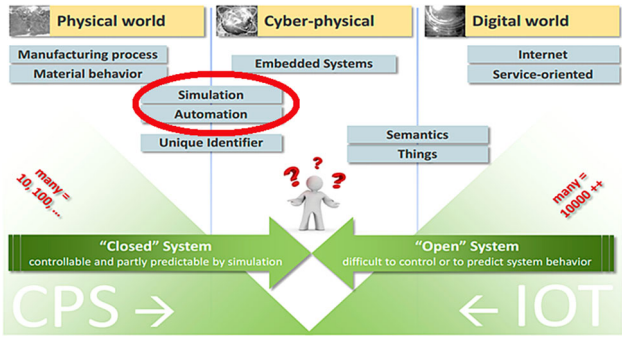

Fig. 2 Two worlds coming together: the physical world and the digital world will converge in the cyber–physical world

between the physical world and the cyber–physical world (Fig. 2).

Interactive simulation techniques can be applied to the industrial scenario in several ways. Global optimisation techniques try to find relationships and correlations between variables measured in the different sensors of the factories. The obtained information is then used to foresee and predict the behaviour of the factory, but also to support 'what-if' scenarios. The 'what-if' analysis is very important for the planning of the long-term and mid-term activities in the factory by answering questions such as: "what is the impact in the production if the factory layout is modified to this one?" or "what is the impact in this specific machining center if we change the laser head to a better technology?".

Answering such questions require knowing very precisely the physical world to transfer that knowledge to the cyber–physical world. In the Industry 4.0 framework, such virtual representation of a real entity is envisioned as a "digital twin". The idea behind this concept is to have a digital entity that behaves exactly (or as closer as possible) as the real entity (Fig. 3). It is important to remark that the expected resemblance goes beyond the physical appearance. The behaviour and functioning of the digital twin is expected to match the reality. But also, the interrelations and collaboration between the digital twins are expected to be part of the simulations.

In the industrial scenarios, the creation of digital twins of production lines composed of a given number of moving and connected machines (robotic arms, conveyors, etc.) is taking off with software suites like Gazebo© or V-Rep©. The complex processes (like the machining processes) are not normally considered and just kinematics of the moving parts are replicated.

In the manufacturing scenarios, the simulation of the machining processes provides measurable benefits for the manufacturing industries, e.g., less wasted energy and resources, and enhanced workers' safety. This work targets the laser cutting processes of planar metal sheets. In a nutshell, this process involves a moving laser head over a metal sheet. The laser beam heats up the targeted point at the sheet

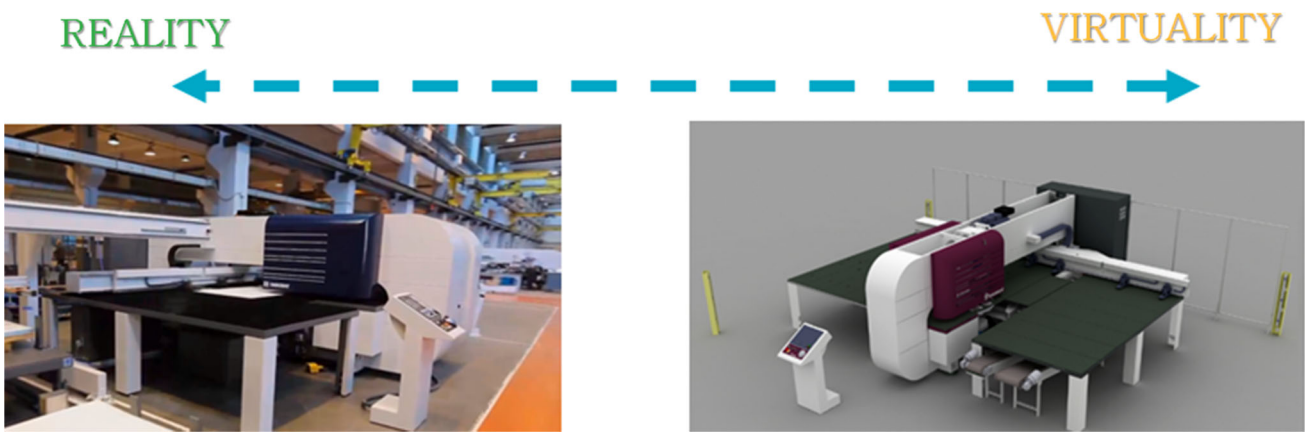

Fig. 3 Digital twins concept: a punching machine in a factory (*left*) and its digital twin (*right*)

till it burns, melts or evaporates. The success of the process depends on the sheet thickness, the sheet physical parameters and the laser parameters. The simulation of the process during the edition, preparation and testing of the NC programs to be sent to the laser machine provides a number of advantages:

1. Optimal configuration of the laser parameters and trajectories can be found without wasting machine time and physical resources.
2. Risk reductions due to the early detection of behavioural patterns and configurations that might produce accidents in the machine.
3. As a overall result, a performance increment of the production line by reducing the non productive machine times for testing the NC programs.

This article addresses the simulation of the heat transfer phenomena in metal sheet laser cutting using different FEM software. This machining process uses a high power laser to melt the metal sheet and to produce the designed part. The heat propagation has to be considered since a bad programming or configuration of the laser parameters could damage the metal sheet rendering useless the produced parts. A review of the current literature in laser cutting simulation is presented in Sect. 2. Section 3 presents the details of the experiment and Sect. 4 presents and discusses the simulation results. Finally, Sect. 5 presents the conclusions and discusses future work.

2 Literature review

A high power density laser locally stimulates the medium (thin metal sheet, in this case) resulting in a high energy input heating the irradiated zone. Reference [2] studies the impact of laser speed on the sheet temperature distribution by running several simulations with different laser speeds. This study was extended to other laser parameters (laser power and spot size) in Refs. [3,4], quantifying the inverse effect of laser speed and laser spot size on the sheet temperature. Reference [5] confirms the statistical significance of the impact of these laser parameters on the resulting sheet temperature using analysis of variance (ANOVA) tests.

The temperature distribution along the sheet in laser cutting processes results in high temperature gradients near the cutting zone. As a consequence, the thermal expansion suffered by the sheet becomes significant and high stresses and strains will affect the quality of the cut. Using thermal stress analysis, Ref. [6] develops a fracture model that aims to predict failure of ceramic plates during laser cutting. Refs. [7,8] combine microstructural analysis with thermal stress analysis in order to study the geometric behavior of the sheet near the cut zone and Ref. [9] study sheet bending using thermal stress analysis and validate the results with experimental data. Experimental data for validation is usually acquired using infrared thermometers (Ref. [3]) or thermocouples (Refs. [7,8,10,11]) in the case of temperature measuring at several sheet locations while Scanning electron microscopy coupled with energy dispersive X-ray spectroscopy (SEM/EDX) is used to extract the structural data at the sheet surface (Refs. [2,7,8,10,11]).

Prediction of material melting is also an important application of heat transfer analysis in laser cutting processes. Reference [11] studies the impact of the kerf size in the resulting temperature distribution demonstrating the importance of material removal in the simulation scenario as results differ significantly from the non-removal of material approach. Latent heat models can be incorporated to simulate the energy exchange during phase change (Refs. [7,8,10,11]) while temperature thresholds are usually defined in order to remove mesh elements with higher temperature values from subsequent timesteps (Refs. [6,12,13]).

Table 1 Summary of this manuscript contributions w.r.t. current state of the art

ID	References	Description	Our approach
1	Refs. [3–5,7–14]	Simulation of laser cutting with commercial software	Comparison of freeware and commercial software for laser cutting
2	Refs. [25,26]	Comparison of FEM software for other engineering applications (not laser cutting)	Comparison of FEM software for laser cutting
3	Refs. [6,12,13]	Material removal using temperature thresholds	Material removal using Boolean operations between contours of the metal sheet and the laser geometries [29]

To simplify the laser cutting model, the aforementioned approaches make several assumptions on the underlying physical phenomena happening at the sheet. These assumptions may not hold during the cutting and more elaborated models with complex interactions have been proposed to increase prediction accuracies. Reference [14] incorporates fluid dynamics to study underwater laser machining and demonstrates how this technique can improve the quality of the resulting cut without affecting much the structural properties of the sheet compared to standard laser machining techniques. Reference [15] proposes a coupled model which considers the interaction between the laser, an assist gas and the melted material on the sheet. This model proves to be superior in accuracy against other models. However, coupling so many interactions in the mathematical model becomes very expensive computationally rendering this model near to useless in industrial applications.

Aside from FEM, other approaches have been also presented for simulation of the laser cutting process. Other numerical alternatives such as the finite difference method (FDM, Refs. [16,17]) or the boundary element method (BEM, Refs. [18,19]) have been successfully implemented producing similar results to FEM. In addition, analytic models and artificial intelligence (AI) models have been also proposed (Refs. [20,21]). However, such analytic models impose a lot of assumptions that limit the application on real case scenarios and AI models limit the domain of the parameter values while requiring a lot of experimental data for training.

2.1 Conclusions of the literature review

This article presents FEM simulations of the heat transfer phenomena during the laser cutting process. Table 1 summarizes the contributions of this manuscript against current state of the art. Most of previous analysis for heat transfer in laser cutting are usually conducted in commercial software such as ABAQUS (Refs. [7–11]) ANSYS (Refs. ([3,4,12–14]) or MSC. MARC (Ref. ([5]). The main contribution of this manuscript in such topic consists of a comparison between a commercial software (ABAQUS) and several freeware FEM software: FreeFem++ (Ref. [22]), FEniCS (Ref. [23]) and MOOSE (Ref. [24]). Comparison studies of FEM software have been presented for some engineering applications such as total knee replacement (TKR) mechanics [25] or the intelligent cross-linked simulations (ICROS) method [26]. However, we have not seen such analysis in the laser cutting literature.

In addition, instead of running 3D simulations we implement the 2D heat transfer model of laser cutting with convection at the surface (Refs. [27,28]) for the simulations. Such model can present some inaccuracies w.r.t. the real phenomenon. Nevertheless, these inaccuracies tend to disappear when the sheet thickness is relatively small which is a reasonable assumption for thin sheets. The results presented in this article consider two scenarios where: (1) there is not material removal and (2) there is material removal. For the latter scenario, the material removal process is classically modelled by removing mesh elements with a temperature-threshold approach (Refs. [6,12,13]). However, in this work the material removal calculation is computed geometrically as Boolean operations between the contours of the metal sheet and the sweep of the moving laser beam that is represented as a vertical cylinder with a fixed diameter. This process is iteratively performed to calculate the sheet geometry at each timestep (Ref. [29]).

3 Methodology

This section discusses the methodology used for the comparison of the different FEM tools. Section 3.1 presents the theoretical model and assumptions for the heat transfer analysis. Section 3.2 discusses some numerical aspects of the chosen FEM tools for comparison. Sections 3.3 and 3.4 discuss the simulation parameters for mesh and time discretization, and the material removal approach which simulates the sheet melting. Finally, Sect. 3.5 briefly discusses the robustness and consistency of the results.

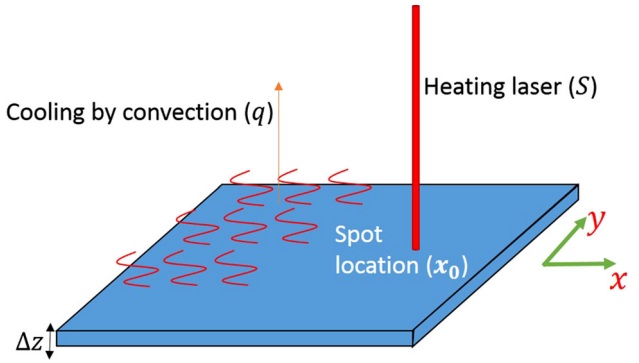

Fig. 4 Scheme of the laser cutting model. A laser passes an amount of energy S at a sheet location $\mathbf{x_0}$ while the surrounding medium cools the sheet due to heat loss q by convection

3.1 Model choice

References [3–7,10,12–16,18,19] use a relativistic heat transfer model (Ref. [30]) since the high relative speed of the laser w.r.t. the sheet affects the heat transfer process. As a result, the relativistic model produces a temperature distribution that differs from the predicted temperature of the classic Fourier heat transfer model. However, we adapt the latter model (classic Fourier) given that the relativistic model imposes a higher degree of implementation complexity in the software used in this manuscript. Therefore, we assume that heat transfer on a 2D metal sheet satisfies the following differential equation (Ref. [27]):

$$\rho c_p \frac{\partial u}{\partial t} - \nabla \cdot (k \nabla u) = S - \frac{q}{\Delta z}. \tag{1}$$

The left side of Eq. (1) contains the energy interactions inside the sheet (i.e. heat conduction) while the right side of the equation contains heat sources (S) and sinks (q). An scheme of the modeled phenomena is presented in Fig. 4. The energy S absorbed by the sheet from the laser is modeled following a gaussian distribution (Ref. [21]):

$$S = \frac{P\,(1-R)}{\pi \sigma^2 \Delta z} \exp\left(-\frac{\left\| \mathbf{x} - \mathbf{x_0} \right\|^2}{\sigma^2} \right), \tag{2}$$

and heat loss q due to natural convection at the sheet surface is modeled by the Newton's law of cooling:

$$q = h(u - u_\infty). \tag{3}$$

Heat loss due to radiation at the surface is not considered. Neumann conditions at the sheet side boundaries are considered adiabatic (i.e. no heat gain/loss at this boundaries) and the initial temperature distribution of the sheet is taken as $u(\mathbf{x}, 0) = u_\infty$.

Table 2 Parameter values for the laser sheet cutting simulation

Parameter	Value
ρ	3950 $\frac{\text{kg}}{\text{m}^3}$
c_p	780 $\frac{\text{J}}{\text{kg K}}$
k	37 $\frac{\text{W}}{\text{m K}}$
R	0
Δz	0.001 m
h	20 $\frac{\text{W}}{\text{m}^2\text{ K}}$
u_∞	293 K
P	3500 W
σ	0.0001 m
v	0.1 $\frac{\text{m}}{\text{s}}$

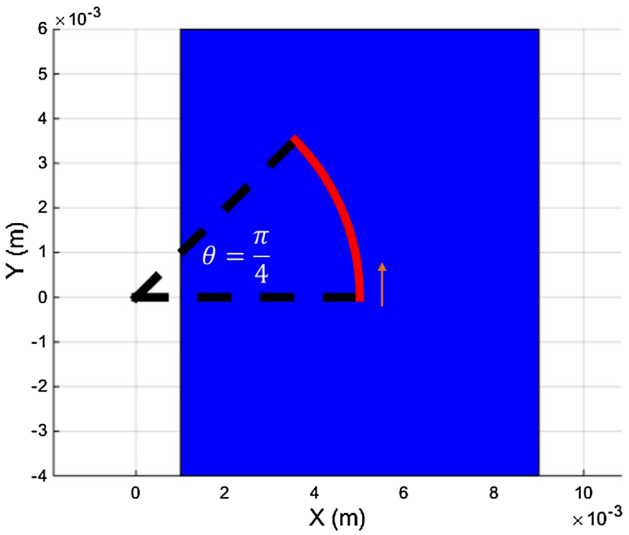

Fig. 5 2D sheet model and laser arc trajectory in a given reference frame

It is well known that Eq. (1) can be solved numerically by FEM. Since the aim of this manuscript is to compare the capabilities of different FEM software for solving this problem, the thermal properties of the sheet ρ, c_p and k are assumed temperature-independent and no phase change is considered. Table 2 presents the parameter values used in the FEM simulations. The chosen values model an alumina tile heated by a CO_2 laser and cooled by natural convection from the surrounding air (Ref. [10]). The sheet dimensions are taken as 0.008 m width × 0.01 m height. Fig. 5 depicts the laser path in a given reference frame. The laser follows an arc trajectory at constant speed (see Table 2) during 0.04 s (which is also the time the complete simulation lasts).

Finally, two different approaches are considered to simulate the laser machining problem:

1. Non-removal of material: in this approach Eq. (1) is solved using FEM while the same geometry is used from

Table 3 FEM software used to carry the simulations

FEM software	Version	Platform
FreeFem++	3.40-2	Windows 64-bits
FEniCS	1.0.0	Windows 32-bits
MOOSE	N/A	Linux 64-bits (VMWare virtual machine on Windows 64-bits)
ABAQUS	6.14 (Intel Compiler 16.0, Visual Studio 2013)	Windows 64-bits

start to end of the simulation. Therefore, the sheet keeps heating in solid phase despite the high temperature that should melt the material. This approach disagrees with the real physical phenomena but allows a comparison of the implemented numerical methods in each software.

2. Material removal: in this approach, elements of the mesh are removed during FEM simulation timesteps according to the laser trajectory as would occur in the real laser machining process. However, instead of the classic approach which removes elements by setting temperature thresholds on elements, the geometry of the sheet is calculated with boolean operations between its contours and the sweep of the moving laser beam defined as a cylinder of a fixed diameter. Section 3.4 discusses this approach in more detail.

3.2 FEM tools

Several freeware and commercial software are used to test the capabilities and the robustness of the solution when simulating the laser cutting phenomena. Table 3 presents a list of the software versions and platforms where the model is implemented. To compare the results between the different software solutions, the relative error E is computed on the whole sheet at a given time:

$$E(\mathbf{x}, t) = \frac{\left\| u(\mathbf{x}, t) - u_{ref}(\mathbf{x}, t) \right\|}{u_{ref}(\mathbf{x}, t)}. \tag{4}$$

The reference temperature u_{ref} is taken as the temperature solution obtained by the ABAQUS software. In addition, the maximum relative error (ME) is computed as follows:

$$ME(t) = \max_{\mathbf{x}} \{E(\mathbf{x}, t)\}, \tag{5}$$

which measures the highest error on the sheet at each timestep. This measure helps to verify experimentally if the solution of the compared software is stable w.r.t. to the reference software or if instead, the error keeps growing through time.

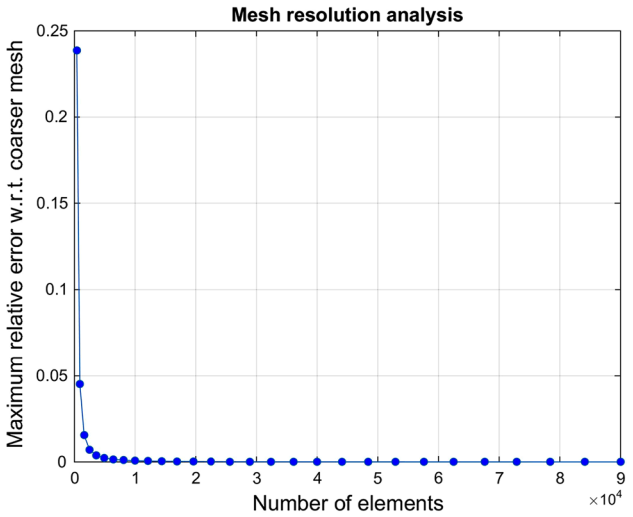

Fig. 6 Maximum relative error of the temperature with respect to the previous temperature solution with a coarser mesh. The laser is pointed to the sheet center during 10^{-4} s

3.3 Problem discretization

In order to keep the simulation conditions as homogeneous as possible between the different software tools, a uniform grid of squared elements is used to discretize the sheet in MOOSE and ABAQUS simulations. Since FreeFem++ and FEniCS only work with triangular meshes, each squared element in the original grid is split into two right triangles for the latter two software tools. Element sizes are critical in laser machinig simulation since the localized high density power source of the laser beam generates high temperature gradients which cannot be adequately captured by coarse meshes. Figure 6 plots the maximum relative error of the temperature with respect to a previous FEM solution with a coarser mesh. In this case, a static laser is irradiated at the center of the sheet during 10^{-4} s. The maximum relative error becomes small enough (and stable) for meshes with more than 10^4 or more elements. This is equivalent to setting element sizes below 10^{-5} m. Therefore, 10^{-5} m size is chosen for the discretization of the sheet in order to guarantee that the solution obtained by the software is an accurate approximation of the analytical solution.

Table 4 Numerical schemes used for approximating Eq. (1) in each software

FEM software	Element type	Element integration	Linear solver
FreeFem++	Triangle (linear)	Gaussian quadrature	Sparse LU decomposition
FEniCS	Triangle (linear)	Linear interpolation	Sparse LU decomposition
MOOSE	Square (bi-linear)	Gaussian quadrature	Preconditioned Jacobian-free Newton–Krylov (PJFNK)
ABAQUS	Square (bi-linear)	Bi-linear interpolation	Sparse Gaussian elimination

In addition, the time is discretized using an implicit finite differences scheme. Each timestep lasts 10^{-3} s. It is reasonable to fix a constant timestep in this case study since Eq. (1) is linear under the previous assumption stating that thermal properties of the sheet are temperature independent. Table 4 presents the numerical options used by each of the software to approximate the solution to Eq. (1). The different software provide a wide variety of values for such options. However, we use the default values as it is the more straightforward approach for the user at implementation time. The variable t is integrated by a backward Euler (implicit) scheme and a Galerkin scheme for linear interpolation is used for integration of the variable $\mathbf{x}$ in all cases.

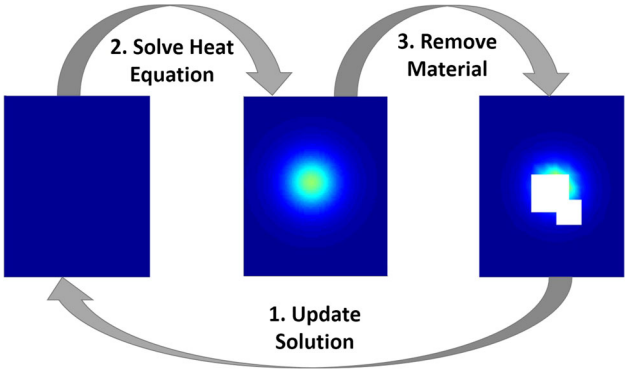

Fig. 7 Scheme used to simulate a timestep of the laser cutting process considering material removal

3.4 Material removal

To simulate material melting from the sheet, elements must be removed from the discretized geometry at each timestep. The most usual approach to do so consists of computing the average temperature on each element and then remove it from the mesh if it surpasses a given threshold (Refs. [6,12,13]). Obviously this task requires additional time resources and can become computationally expensive when simulating manufacturing scenarios.

Instead of the usual approach, a radius threshold from the laser spot location can be set if the kerf size is known. This corresponds to removing elements inside a ball of radius $\frac{\varepsilon}{2}$ centered at $\mathbf{x_0}$. Therefore, for each timestep three actions must be taken: (1) update the last step solution (temperature and geometry), (2) solve heat equation for current timestep and (3) remove sheet material. Figure 7 illustrates this simulation approach from a given timestep. For simplification purposes, the kerf width is taken as $\varepsilon = 2\sigma$. The material removal process is calculated by subtracting the sweep of the moving laser beam from the sheet representation (Ref. [29]). The resulting contours are converted into the mesh files for the FreeFem++ and ABAQUS solvers.

3.5 Consistency verification

According to [31], if the laser path is parallel to the x axis, the temperature distribution of the 2D sheet during laser cutting

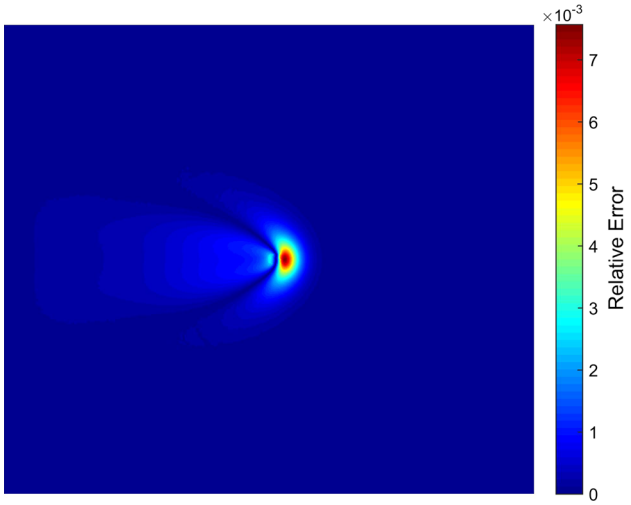

Fig. 8 Relative error distribution of the FEM solution w.r.t. the analytic solution [31] for a linear laser path

(without convection nor material removal) can be expressed analytically as a Fourier series:

$$u = u_\infty + \frac{4}{\rho c_p a b} \times \sum_{i,j}^{\infty} \left[\int_0^t \int_\Omega S(\mathbf{x}, \tau) \mathbb{X}_i(x) \mathbb{Y}_j(y) e^{-\omega_{ij}(t-\tau)} \, \mathrm{d}\Omega \, \mathrm{d}\tau \right] \times \mathbb{X}_i(x) \mathbb{Y}_j(y), \quad (6)$$

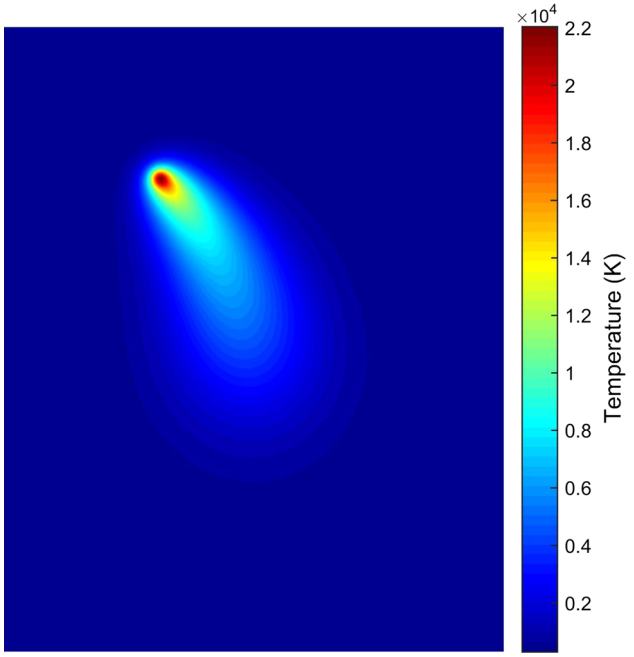

Fig. 9 Temperature distribution without material removal at $t = 0.04$ s obtained by ABAQUS

where $\mathbb{X}_i$ and $\mathbb{Y}_j$ are the eigenfunctions of the Laplacian $\nabla \cdot \nabla$ on the sheet and ω_{ij} are their corresponding eigenvalues defined as:

$$\mathbb{X}_i(x) = \sin \frac{i\pi x}{a}$$
$$\mathbb{Y}_j(y) = \sin \frac{j\pi y}{b}$$
$$\omega_{ij} = \frac{k\pi^2}{\rho c_p}\left(\frac{i^2}{a^2} + \frac{j^2}{b^2}\right). \tag{7}$$

We use the FEM software to solve this problem and compare the results with Eq. (6) in order to check the accuracy of the results and the validity of the implemented model. The relative error distribution of the FEM solution with respect to the analytic solution is presented in Fig. 8. The maximum relative error is located at the laser front and it is below 0.8 %. The FEM solution is therefore a good approximation of the 2D laser cutting heat transfer problem.

4 Results and discussion

This section presents and discusses the simulation results obtained by the different FEM software. Results for the non-removal of material case are presented in Sect. 4.1 and results for the material removal case are presented in Sect. 4.2.

4.1 Results without material removal

Figure 9 plots the temperature distribution on the sheet after the laser has drawn the trajectory depicted in Fig. 5 at $t = 0.04$ s. A maximum temperature of ≈22,000 K is achieved exactly where the laser spot is located at such timestep and the laser trail on the sheet has been slightly cooled due to convection. The arc trajectory aims to resemble real laser machining processes where the laser trajectory is nonlinear and does not allow simplification through a symmetry axis which is exploited by other laser cutting analysis in the literature (e.g. Refs. [3–7,10,12–16,18,19]).

Figure 10 plots the relative error distribution of the freeware software (FreeFem++, FEniCS, MOOSE) solutions w.r.t. the ABAQUS solution shown in Fig. 9. The FreeFem++ and FEniCS solution show a similar error distribution pattern while the MOOSE solution plots a very different pattern. These patterns behaviors is mainly associated to the elements used to compute the solution since FreeFem++ and FEniCS used the same triangular elements while MOOSE used squared elements as shown in Table 4. In all the cases the

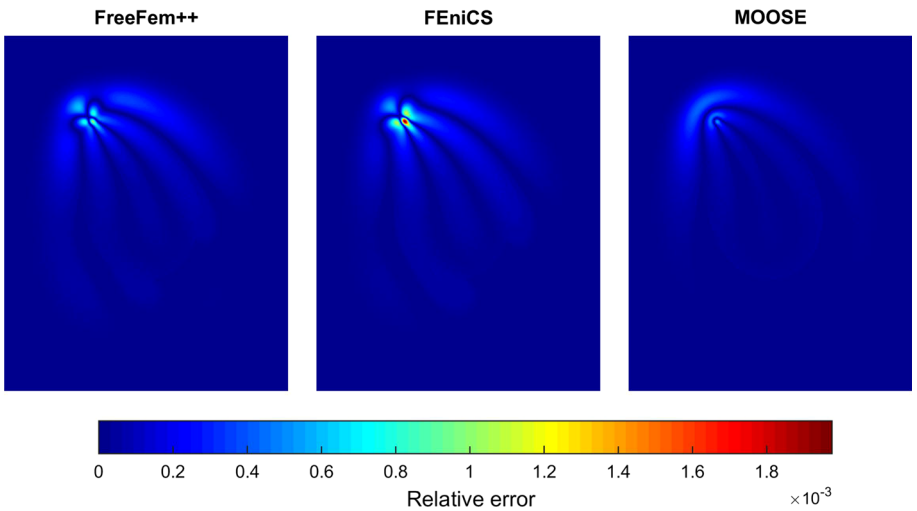

Fig. 10 Relative error distribution of the temperature field obtained by FreeFem++, FEniCS and MOOSE respectively w.r.t. ABAQUS result at $t = 0.04$ s

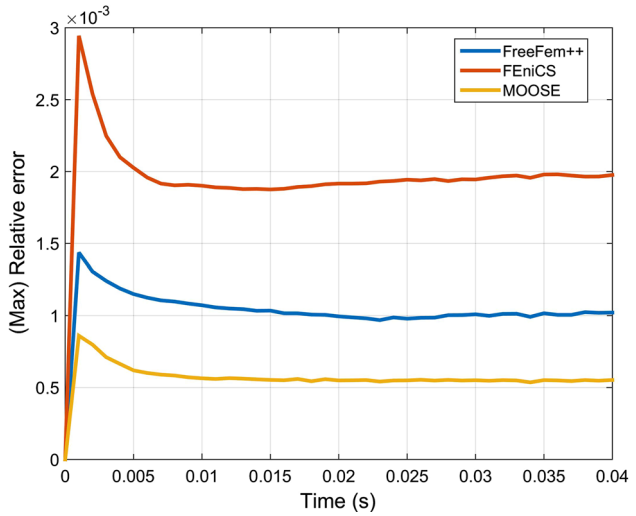

Fig. 11 Maximum relative error evolution of the temperature field through time for the freeware software w.r.t. ABAQUS

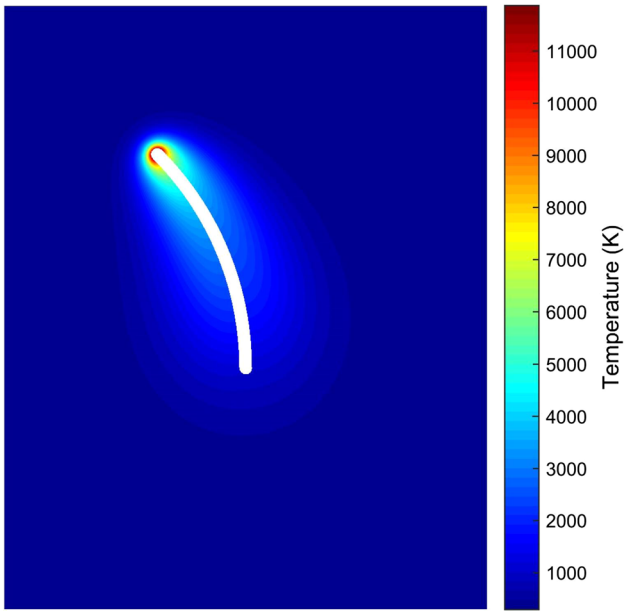

Fig. 12 Temperature distribution with material removal at $t = 0.04$ s obtained by ABAQUS

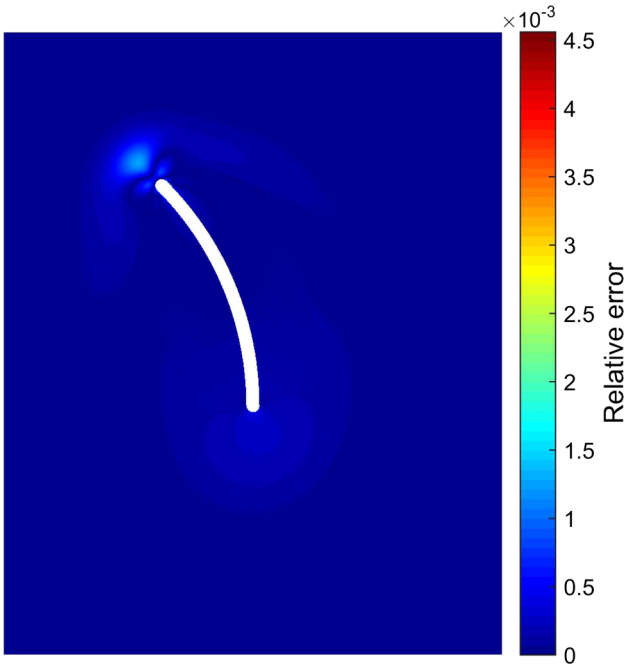

Fig. 13 Relative error distribution of the FreeFem++ temperature field result (with material removal) w.r.t. ABAQUS result at $t = 0.04$ s

error is concentrated at the laser spot, followed by the laser trail and the cutting front respectively. Of course, this error distribution is expected as the implementation of the integration scheme (e.g. linear interpolation or interpolation by quadrature) at each element differs between software introducing approximation differences at the high temperature gradient zones. In addition, numerical errors also arise due to the linear solver used by each software. Figure 11 plots the maximum relative error evolution through the simulation for the different software tools. The maximum error is at tolerable levels ($ME \leq 0.3$ %) and stays stable regardless the software. MOOSE solution displays a better performance (less error) w.r.t. ABAQUS. Again, this may be due to the fact that the elements used in MOOSE and ABAQUS simulations are the same while FreeFem++ and FEniCS employ different elements.

4.2 Results with material removal

Following the methodology described in Sect. 3.4, Fig. 12 presents the temperature distribution on the sheet at $t = 0.04$ s. In this case, the material melted by the laser is removed in the simulation. As a consequence, the maximum temperature achieved considering material melting ($\approx$12,000 K) is significantly lower than the maximum temperature achieved without the material removal approach ($\approx$22,000 K, Fig. 9). This difference illustrates the importance of material removal in laser machining simulations since melted elements that are not removed accumulate heat which will propagate through conduction to the non-melted zones, resulting in an overestimation of the temperature.

Figure 13 plots the relative error distribution of the temperature computed by the FreeFem++ software w.r.t. the ABAQUS result (Fig. 12) considering material removal. In this case the maximum error concentrates at the cutting front which does not surpasses the 0.5 %. Figure 14 plots the maximum relative error evolution of the FreeFem++ temperature distribution w.r.t. the ABAQUS solution with material removal. The maximum relative error *ME* is stable and does not exceeds the 1.2 %. As discussed before, this error is

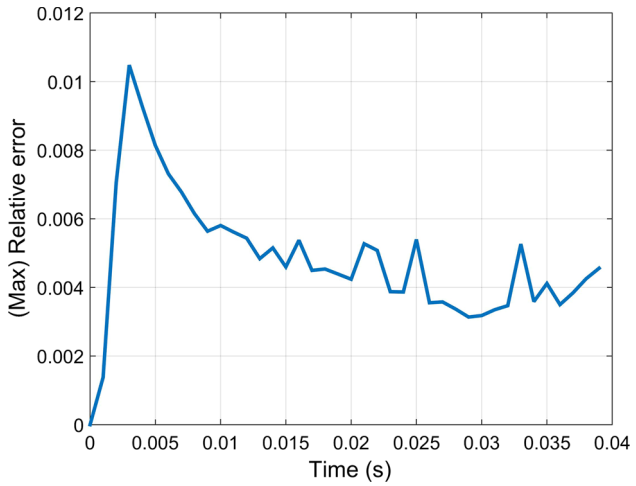

Fig. 14 Maximum relative error evolution of the temperature field (with material removal) through time of FreeFem++ solution w.r.t. ABAQUS solution

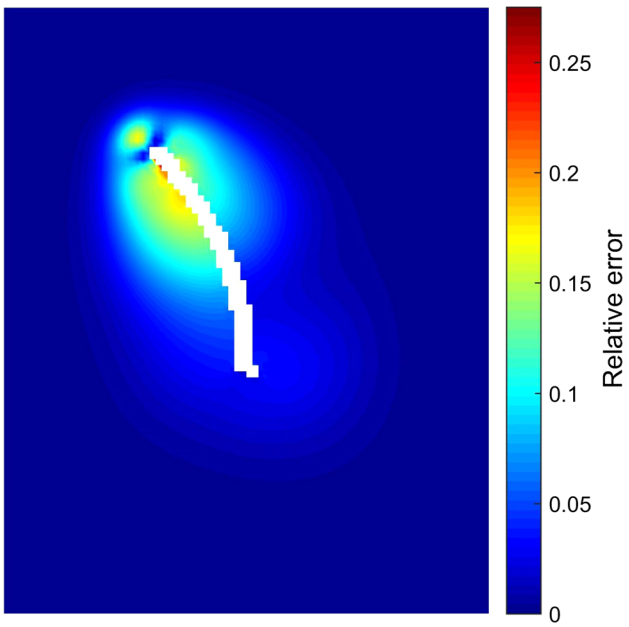

Fig. 15 Relative error distribution of the temperature field (with material removal) obtained by FreeFem++ w.r.t. ABAQUS result at $t = 0.04$ s for a coarse mesh

mainly due to differences in the integration schemes and numerical solvers as well as the type of elements used by each software.

Figure 15 presents the error distribution of the temperature computed by FreeFem++ w.r.t. ABAQUS temperature for a coarse mesh (10^{-4} m $\times$ 10^{-4} m element size). For coarse meshes, both software tools compute very different temperature distributions as the error reaches levels of ≈28 %. Simulation results in this case are very different from the real world scenario since the integration schemes for each element cannot approximate accurately the laser effects. This

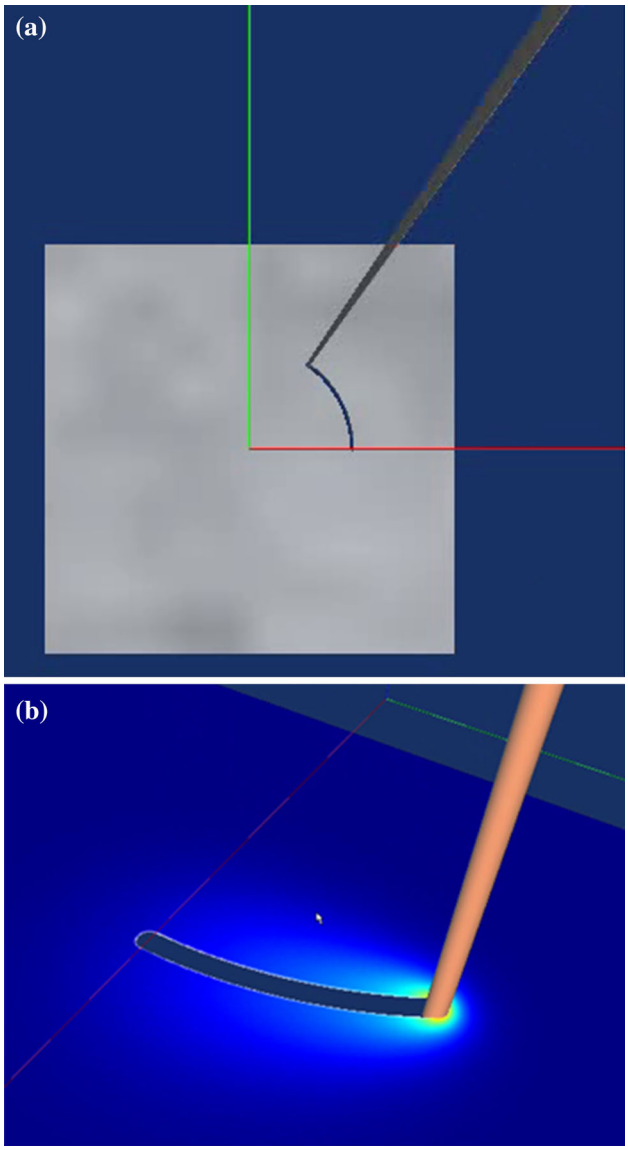

Fig. 16 Integration of the FEM results in the machining cutting simulator. **a** The laser beam cuts geometrically the metal sheet. **b** A isometric 3D view of the metal sheet textured with the FEM results instead of the metal texture shown in **a**

result reaffirms the importance of the mesh resolution in laser machining simulations as seen in Fig. 6.

5 Conclusions

This article presented a comparison of FEM simulation results of FreeFem++, FEniCS, MOOSE and ABAQUS. For the comparison, a 2D classic heat transfer model was used to allow a nonlinear (arc) laser trajectory. In addition, the thermal properties of the sheet were considered independent of the temperature. Two study cases were tested: (1) laser cutting simulation without material removal and (2) laser

cutting simulation with material removal. For the latter one, the material removal process was geometrically computed as Boolean operations between the sheet's contours and the sweep of the moving laser beam, defined as a cylinder of fixed diameter. Figure 16 presents a preliminary integration of the FEM simulation results in the laser cutting simulator.

Under an adequate meshing, the simulation results thrown by the freeware software did not differ much from the reference (ABAQUS) result, with an error below 0.3 % for the non-removal of material case and 1.2 % for the material removal case. The error also proved to be stable through time which guarantees accuracy of the results for the transient problem regardless the FEM tool used. A coarse mesh comparison also was presented resulting in an error close to 27 %. The increase in the error measured is due to the difference between integration schemes between software implementations which approximate the heat source (laser) inside each element. This error increase indirectly illustrates the importance of the mesh resolution size in the accuracy of the obtained solutions as they tend to converge to the same solution when the mesh becomes denser.

5.1 Ongoing work

The temperature independence assumption of the sheet physical properties may not be an adequate assumption in the laser machining process since the high temperature changes could arise significant changes in such physical properties. Ongoing work addresses this problem by considering material nonlinearities. By linear interpolation of the thermal properties and selective time stepping, Eq. (1) can be solved by an iterative solver.

In addition, mesh resolution has proven to be a key factor for obtaining accurate results. Therefore, dynamic adaptive re-meshing or multiresolution techniques (e.g. [32]) should be accounted for simulation of bigger (spatial and time) domains. Future work also aims to couple the heat equation with a strain/stress model to analyse the structural changes of the sheet due to thermal effects.

Finally, a relativistic heat transfer model (Ref. [30]) takes into account the effect of the relative high speed of the laser source w.r.t. the sheet as well as the inclusion of a heat transfer speed bound which becomes significant with high temperature gradients according to the theory of relativity. Implementation of such model could therefore provide a more accurate prediction of the temperature field on the sheet while allowing a better understanding of the underlying physical phenomena.

Acknowledgments This research has been funded by the CAD CAM CAE Research Group and the College of Engineering at Universidad EAFIT, Colombia.

References

1. Posada, J., Toro, C., Barandiaran, I., Oyarzun, D., Stricker, D., De Amicis, R., Pinto, E., Eisert, P., Dollner, J., Vallarino, I.: Visual computing as a key enabling technology for industrie 4.0 and industrial internet. IEEE Comput. Graph. **35**(2), 26–40 (2015). doi:10.1109/MCG.2015.45
2. Yilbas, B.S., Arif, A.F.M., Abdul Aleem, B.J.: Laser cutting of rectangular blanks in thick sheet steel: effect of cutting speed on thermal stresses. J. Mater. Eng. Perform. **19**(2), 177–184 (2010). doi:10.1007/s11665-009-9477-8
3. Song, W.Q., Xu, W.J., Wang, X.Y., Meng, J.B., Li, H.Y.: Numerical simulation of temperature field in plasma-arc flexible forming of laminated-composite metal sheets. Trans. Nonferr. Metals Soc. **19**, s61–s67 (2009). doi:10.1016/S1003-6326(10)60246-4
4. Joshi, A., Kansara, N., Das, S., Kuppan, P., Venkatesan, K.: A study of temperature distribution for laser assisted machining of ti-6al-4 v alloy. Proc. Eng. **97**, 1466–1473 (2014). doi:10.1016/j.proeng.2014.12.430
5. Tagliaferri, F., Leopardi, G., Semmler, U., Kuhl, M., Palumbo, B.: Study of the influences of laser parameters on laser assisted machining processes. Proc. CIRP **8**, 170–175 (2013). doi:10.1016/j.procir.2013.06.084
6. Akarapu, R., Li, B.Q., Segall, A.: A thermal stress and failure model for laser cutting and forming operations. J. Fail. Anal. Prev. **4**(5), 51–62 (2004). doi:10.1361/15477020420756
7. Yilbas, B.S., Akhtar, S.S.: Laser bending of metal sheet and thermal stress analysis. Opt. Laser Technol. **61**, 34–44 (2014). doi:10.1016/j.optlastec.2013.12.023
8. Akhtar, S.S.: Laser cutting of thick-section circular blanks: thermal stress prediction and microstructural analysis. Int. J. Adv. Manuf. Tech. **71**(5–8), 1345–1358 (2014). doi:10.1007/s00170-013-5594-5
9. Nadeem, Q., Na, S.J.: Deformation behavior of laser bending of circular sheet metal. Chin. Opt. Lett. **9**(5), 051402 (2011). doi:10.3788/COL201109.051402
10. Yilbas, B.S., Akhtar, S.S., Karatas, C.: Laser straight cutting of alumina tiles: thermal stress analysis. Int. J. Adv. Manuf. Tech. **58**(9–12), 1019–1030 (2012). doi:10.1007/s00170-011-3439-7
11. Akhtar, S., Kardas, O.O., Keles, O., Yilbas, B.S.: Laser cutting of rectangular geometry into aluminum alloy: Effect of cut sizes on thermal stress field. Opt. Laser Eng. **61**, 57–66 (2014). doi:10.1016/j.optlaseng.2014.04.016
12. Nyon, K.Y., Nyeoh, C.Y., Mokhtar, M., Abdul-Rahman, R.: Finite element analysis of laser inert gas cutting on inconel 718. Int. J. Adv. Manuf. Tech. **60**(9–12), 995–1007 (2012). doi:10.1007/s00170-011-3655-1
13. Yan, Y., Ji, L., Bao, Y., Chen, X., Jiang, Y.: CO_2 laser high-speed crack-free cutting of thick-section alumina based on close-piercing lapping technique. Int. J. Adv. Manuf. Tech. **64**(9–12), 1611–1624 (2013). doi:10.1007/s00170-012-4127-y
14. Yan, Y., Li, L., Sezer, K., Wang, W., Whitehead, D., Ji, L., Bao, Y., Jiang, Y.: CO_2 laser underwater machining of deep cavities in alumina. J. Eur. Ceram. Soc. **31**(15), 2793–2807 (2011). doi:10.1016/j.jeurceramsoc.2011.06.015
15. Gross, M.S.: On gas dynamic effects in the modelling of laser cutting processes. Appl. Math. Model. **30**(4), 307–318 (2006). doi:10.1016/j.apm.2005.03.021
16. Modest, M.F.: Three-dimensional, transient model for laser machining of ablating/decomposing materials. Int. J. Heat Mass Transf. **39**(2), 221–234 (1996). doi:10.1016/0017-9310(95)00134-U
17. Modest, M.F.: Laser through-cutting and drilling models for ablating/decomposing materials. J. Laser Appl. **9**(3), 137–145 (1997). doi:10.2351/1.4745453

18. Kim, M.J.: Transient evaporative laser-cutting with boundary element method. Appl. Math. Model. **25**(1), 25–39 (2000). doi:10.1016/S0307-904X(00)00034-2
19. Kim, M.J.: Transient evaporative laser cutting with moving laser by boundary element method. Appl. Math. Model. **28**(10), 891–910 (2004). doi:10.1016/j.apm.2004.03.001
20. Dubey, A.K., Yadava, V.: Laser beam machining: a review. Int. J. Mach. Tool. Manu. **48**(6), 609–628 (2008). doi:10.1016/j.ijmachtools.2007.10.017
21. Parandoush, P., Hossain, A.: A review of modeling and simulation of laser beam machining. Int. J. Mach. Tool. Manu. **85**, 135–145 (2014). doi:10.1016/j.ijmachtools.2014.05.008
22. Hecht, F.: New development in FreeFem++. J. Numer. Math. **20**(3–4), 251–265 (2012). doi:10.1515/jnum-2012-0013
23. Logg, A., Mardal, K.A., Wells, G.: Automated Solution of Differential Equations by the Finite Element Method, Lecture Notes in Computational Science and Engineering, vol. 84. Springer, Heidelberg (2012)
24. Gaston, D., Newman, C., Hansen, G., Lebrun-Grandi, D.: MOOSE: a parallel computational framework for coupled systems of nonlinear equations. Nucl. Eng. Des. **239**(10), 1768–1778 (2009). doi:10.1016/j.nucengdes.2009.05.021
25. Strickland, M.A., Arsene, C.T.C., Pal, S., Laz, P.J., Taylor, M.: A multi-platform comparison of efficient probabilistic methods in the prediction of total knee replacement mechanics. Comput. Method. Biomech. **13**(6), 701–709 (2010). doi:10.1080/10255840903476463
26. Roith, B., Troll, A., Rieg, F.: Integrated finite element analysis (FEA) in three-dimensional computer aided design programs (CAD)—overview and comparison. In: Bocquet J.C. (ed.) Proceedings of ICED 2007, the 17th international conference on engineering design, pp. 1–12. The Design Society (2007)
27. Pietro, P.D., Yao, Y.L.: A numerical investigation into cutting front mobility in CO_2 laser cutting. Int. J. Mach. Tool. Manu. **35**(5), 673–688 (1995). doi:10.1016/0890-6955(95)93037-7
28. Aloke, R., Girish, V., Scrutton, R.F., Molian, P.A.: A model for prediction of dimensional tolerances of laser cut holes in mild steel thin plates. Int. J. Mach. Tool. Manu. **37**(8), 1069–1078 (1997). doi:10.1016/S0890-6955(96)00090-9
29. Moreno, A., Segura, A., Arregui, H., Posada, J., Ruíz de Infante, A., Canto, N.: Using 2d contours to model metal sheets in industrial machining processes. In: De Amicis R. , Conti G. (eds.) Future Vision and Trends on Shapes, Geometry and Algebra. Springer Proceedings in Mathematics Statistics, vol. 84, pp. 135–149. Springer, London (2014)
30. Ali, Y., Zhang, L.: Relativistic heat conduction. Int. J. Heat Mass Transf. **48**(12), 2397–2406 (2005). doi:10.1016/j.ijheatmasstransfer.2005.02.003
31. Jiang, H.J., Dai, H.L.: Effect of laser processing on three dimensional thermodynamic analysis for HSLA rectangular steel plates. Int. J. Heat Mass Transf. **82**, 98–108 (2015). doi:10.1016/j.ijheatmasstransfer.2014.11.003
32. Boffy, H., Baietto, M.C., Sainsot, P., Lubrecht, A.A.: Detailed modelling of a moving heat source using multigrid methods. Tribol. Int. **46**(1), 279–287 (2012). doi:10.1016/j.triboint.2011.06.011